



*Research paper*

## **Simulation the Effects of Fiber on the Poisson's Ratio of Self-Compacting Concrete**

**Hamoon Fathi<sup>1\*</sup>, Mohammad Yousefinezhad<sup>2</sup>**

1\*- Department of Civil Engineering, Islamic Azad University, Sanandaj branch, IRAN;

2- Department of Civil Engineering, Islamic Azad University, Roudehen branch, IRAN;

Received: 08 September 2023; Revised: 06 October 2023; Accepted: 19 October 2023; Published: 22 October 2023

### **ABSTRACT**

The present paper studies experimental research on the effects of fiber on the strain and the Poisson's ratio of self-compacting concrete (SCC). The experiment was carried out on 48 cubic concrete samples and 68 standard cylindrical samples of 4 different mixes with compressive strengths of 25, 28, 30, and 33 MPa. The percentage of fiber in the mixes increases from 0 to 12. Axial and lateral strains of the samples were calculated simultaneously, with respect to the stress exerted by uniaxial compressive loading. Having compared the stress-strain curves for axial and lateral strain, Poisson's ratios were calculated by taking the number of the loadings into account. One of the implications of the results was that the ratio of the inner area in lateral stress-strain curve to those in axial stress-strain curve relate to the square of Poisson's ratio in the same percent of fiber. At the end, with respect to the concrete's compressive strength and percentage of fibers, an integrated model was formulated for Poisson's ratio of fiber SCC under compressive loading. The results show that an increase in fiber (only 2%) causes a significant increase in Poisson's ratio (more than 5%) after the second compressive loading. Also, the third lateral strain provides maximum strength in all self-compacting concrete mixes.

**Keywords:** fiber, Poisson's ratio, axial strain, lateral strain, self-compacting concrete.

*Cite this article as: FATHI, H., & Yousefinezhad, M. (2023). Simulation the Effects of Fiber on the Poisson's Ratio of Self-Compacting Concrete. Civil and Project, 5(7), 38-46. <https://doi.org/10.22034/cpj.2023.419946.1223>*

ISSN: [2676-511X](https://doi.org/10.22034/cpj.2023.419946.1223) / Copyright: © 2023 by the authors.

**Open Access:** This article is licensed under a Creative Commons Attribution 4.0 International License, which permits use, sharing, adaptation, distribution and reproduction in any medium or format, as long as you give appropriate credit to the original author(s) and the source, provide a link to the Creative Commons licence, and indicate if changes were made. The images or other third party material in this article are included in the article's Creative Commons licence, unless indicated otherwise in a credit line to the material. If material is not included in the article's Creative Commons licence and your intended use is not permitted by statutory regulation or exceeds the permitted use, you will need to obtain permission directly from the copyright holder. To view a copy of this licence, visit <https://creativecommons.org/licenses/by/4.0/>

**Journal's Note:** CPJ remains neutral with regard to jurisdictional claims in published maps and institutional affiliations.

\*Corresponding author E-mail address: Email: [Hamoon.fathi@gmail.com](mailto:Hamoon.fathi@gmail.com)

## **1. Introduction**

SCC has been widely used due the simplicity of its production and pumping condition and its compression because of its weight. Although the behavior of SCC is expected not to be different from that of common concrete, controlling its specification and seismic behavior is necessary for accurate designing. Much research has been performed on studying concrete behavior under and uniaxial compressive loading (Ayhan et al., 2013; Crambuer et al., 2013; Mi et al., 2023).

the effect of polypropylene fibers on concrete compressive strength and bonding strength between concrete and GFRP rebar was investigated experimentally. The results showed that the bond resistance between the polypropylene fiber-reinforced concrete and GFRP rebar increased with the increase in the number of fibers. (Mohsenian et al., 2023; Wei et al., 2019; Huang et al., 2020)

One of the mechanical properties of materials is Poisson's ratio. It deals with the way materials are deformed with respect to the loading type in a specified behavioral range. Theoretically, Poisson's ratio is within the range of -1 to 0.5. While most of the natural materials have a positive Poisson's ratio, some polymeric materials with a negative Poisson's ratio have been identified (Friis et al., 1988; Lakes, 1987; Zeng et al., 2023). Poisson's ratio is one of the crucial properties in designing. It is within the range of 0.1 to 0.3 for most concretes. Much research has dealt with the Poisson's ratio of concretes with various properties. For instance, compressive strength influences concrete Poisson's ratio. A type of concrete with a higher compressive strength has a lower Poisson's ratio (Gu, 2022; Swamy, 1971; Wany and Qingbin, 2007). In fact, brittle materials have a lower Poisson's ratio. Poisson's ratio is related to the modulus of elasticity, and some other properties of concretes. Many studies have been carried out to investigate these relations, and many equations have been formulated to calculate them. Poisson's ratio is related to concrete demolition rate, and it changes as it cracks and is demolished. In fact, Poisson's ratio or its rate of change can serve as criteria for determining the demolition rate of concrete or other materials (Azoti et al., 2013; Sideris et al., 2004). It relates to the structure of materials and the way particles are arranged. Aggregate size, the ratio of mortar's compressive strength to aggregates, gradation chart, additives and the fiber used in the concrete affect its main properties and the way cracks are spread. In fact, the passage of cracks along or within the aggregates influences the rates of reversible strains and permanent strains, hence changing Poisson's ratio. Initial cracks that have been created due to loading, chemical factors, or concrete shrinkage spread as external factors, temperature or loading history change. Fatigue loading is a low intensity loading. Another factor affecting the speed at which cracks spread is the speed of loading or strain rate (Xie et al., 2023; Gusatis, 2011; Asprone et al., 2012). The present study was carried out due to the importance of determining Poisson's ratio as one of mechanical properties of concrete, small cracks, and permanent strains as a result of loading history as well as the wide use of SCC. Hence, this laboratory study analyzed Poisson's ratio variations and axial and lateral strains due to compressive loading on SCC, but fiber can change the lateral strain and these results introduce to design programs.

## 2. Materials and method

The present study investigated the effects of repeated uniaxial compressive loading on the Poisson ratio of fiber SCC. The fiber SCC specimens were compacted under their self-weight with very little vibrations.

### 2.1. Mixtures

Constituents of concrete mixes such as micro silica, plasticizer and crushed stone aggregates were collected from local materials (Table 1). Portland cement type was a normal type. Micro silica was a type of silica fume and plasticizer called MN 128h.

**Table 1 . Materials qualifications**

Materials name	Materials type	Qualifications
Aggregate	Crashed stone	Bulk : 1650 kg/m <sup>3</sup>
Water	Normal	PH : 7
fiber	PPP	L : 10mm
Additives	Micro silica	Density : 2110 kg/m <sup>3</sup>
	Plasticizer	Density : 1200 kg/m <sup>3</sup>

The concrete is fiber SCC (Table.2). Concrete samples with four different mix designs have four compressive strengths (25, 28, 30 and 33 MPa). fiber with four different percentages (0%, 4%, 8%, and 12%) is added to the mixes. These items affect the compressive strength and slump flow.

**Table 2. Self-compacting concrete Mixes**

Groups name	Cement percentage			Gravel
	plasticizer	fiber	water	Sand
FSCC 1	3 %	2 %	36 %	0.9
FSCC 2	3 %	4 %	33 %	0.9
FSCC 3	3 %	6 %	31 %	0.9
FSCC 4	3 %	8 %	29 %	0.9

## 2.2. Construction

Aggregates, cement, and supplementary cementitious materials were mixed for 1 minute. Afterwards, a combination of water and plasticizer was added to the mix. Having mixed the materials for 1 minute, the remaining water was added. After 2 minutes, slump flow of the samples was controlled in order to ensure their self-compaction. Potentially, the concrete mixer can make 12 samples of standard cylindrical concretes in each mixing session. Having controlled the materials, they were poured in molds. After 24 hours, the concretes were removed from their molds and were completely placed in a mix of water and a little lime.

## 2.3. Specimens

A number of 48 cubic samples (150 mm) and 68 standard cylinders (150\*300) were produced and investigated. The produced samples were categorized under four categories with respect to their compressive strength. The compressive strengths of cylindrical concrete samples were 25, 28, 30, and 33 MPa, with each group having 12 cylindrical concrete samples. In order to determine the appropriate mixing pattern, 48 cubical samples were made as prototypes (Fig. 1). After making sure about the prototypes, cylindrical samples were made. Three samples in each category were used for studying uniform compressive axial loading and the 3 others were used for studying the modulus of elasticity. Moreover, the last 8 samples of each category were put under uniaxial compressive loading. The axial and lateral strains of each sample were calculated for uniform and uniaxial compressive loading with respect to the amount of applied load.



**Fig. 1:** cubical samples

## 2.4. Test machine

In order to perform the experiments accurately and get to appropriate results, many strain gauges with micron accuracy were used. Instruments were designed in a way that in every loading session, the strain along with the axial loading and the strain perpendicular to the loading axis were calculated for the SCC under uniaxial compressive loading. In order to determine the axial strain, 3 sensors parallel to the normal vector of cylinder section were located around the cylindrical sample. The averages of the three readings were defined as section center strain. Moreover, a metal chain was placed in the middle of the sample and around the cylinder. A soft spring was used for fastening and opening the chain. There were 2 handles on the chain which were connected to 2 sensors at their ends (Fig. 2). The cylinder's perimeter increased as the sample deformed laterally. The chain's opening expanded as the perimeter increased and sensors captured the changes in the angles.

Fig. 2 illustrates the map and location of strain gauges, handles, and other items. Furthermore, the position of the sample and the lateral strain gauge are shown in Fig. 2. The handle and the strain gauges can simultaneously calculate the axial and lateral strains at every moment. Poisson's ratio was determined by ratio of the axial strain to the lateral strain.



**Fig. 2:** The location of lateral and axial strain gauges.

1- Cylindrical sample; 2- Flexible joint; 3- Steel chain; 4- Strain gauge jaw; 5- Support; 6- Mobile lever; 7- Strain gage; 8- Vertical strain gage place; 9- Horizontal strain age framework; 10- Control bolt; 11- Main body;

## 2.5. Loading method

Two types of loading were used in the study. Uniform compressive axial loading with a constant speed in the quasi-static limit was performed in order to determine limit of stress-strain curve, and the maximum compressive strength of the samples. Unilateral compressive uniaxial compressive loading with a constant speed in increasing load was applied to the samples (Fig. 3). The load was increased in every loading session by 60%  $f'_c$  and repeated 5 time. As the loading reached its compressive maximum, it was decreased.

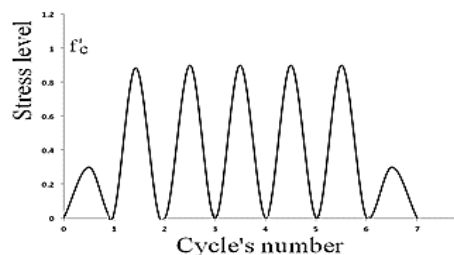


**Fig. 3:** compressive uniaxial compressive loading curve

Fig. 3 illustrates loading and unloading within the compressive limit. First, the compressive strengths of 3 samples were calculated using uniform unilateral compressive loading. Their average was defined as the maximum compressive strength ( $f'_c$ ). The uniaxial compressive strain increased gradually by 60% according to the value of  $f'_c$ . Unloading continued until just before the disconnection of compression jack from the cylindrical sample and produced fiber effects on lateral strain in each time. Afterwards, loading started again. This was done due to the fact that as a result of permanent strains, concrete does not return to its original position. When the compressive stress reaches the maximum strain strength of the concrete, the sample breaks. At this moment, the system shows a fall in force and stress. After that point, loading is reversed and gradually decreased.

### 3. Discussion and results

Simultaneous study of stress and strain makes it possible to plot axial and lateral stress-strain curve. In order to study the effects of uniaxial compressive loading on Poisson's ratio accurately and repeated 5 time for finding fiber effects, lateral and axial strains must be measured simultaneously. While Poisson's ratio is a constant value for a concrete sample in uniform compressive loading, the ratio of lateral strain to longitudinal strain changes as the concrete cracks in each loading. The factors affecting the behavior of strain increasing or decreasing pattern are the way cracks spread, open or close as well as the decrease in compressive strength.

#### 3.1. Mechanical properties of SCC specimens

In order to ensure the self-compaction of samples, the flowing slump of the samples was controlled after mixing. Three samples from each concrete production session were put under uniform unilateral compressive loading. Their average was defined as compressive strength. Three samples were also studied in order to determine the modulus of elasticity (Table 4).

**Table 4.** The mechanical properties of concrete samples

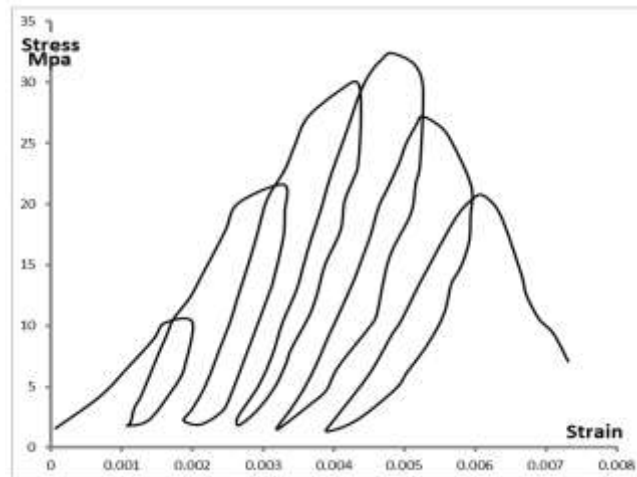
Groups name	Slump flow	Compressive strength	Poisson's ratio
SCC 1	68 cm	25 MPa	0.175
SCC 2	63 cm	28 MPa	0.174
SCC 3	60 cm	30 MPa	0.172
SCC 4	56 cm	33 MPa	0.169

Table 4 shows the flowing slump, compressive strength and Poisson's ratio. As the compressive strength of the sample increased, the modulus of elasticity increased while Poisson's ratio decreased. These results indicate that samples become more brittle as their compressive strength increases. Moreover, a concrete with a brittle behavior shows a lower Poisson's ratio.

#### 3.2. Stress-strain curve

The axial and lateral strains of the samples were studied with respect to the applied stress and the type of loading. Fig. 4 and 5 show the lateral and axial stress-strain curves of SCC samples under uniaxial compressive loading. Fig. 4 shows the axial stress-strain curve of SCC3 concretes. The compressive strength of SCC3 in uniform loading was 30 MPa. Because of the cracks made as a result of 3 repeated loading under the peak point of the curve, their compressive strength decreased to 28 MPa.

Reloading branch before the peak point increased the slope of loading branch which was caused by permanent strains in the concrete. Furthermore, reloading branches after the peak point decreased loading slope which was caused by the deep cracks in the samples.



**Fig. 4:** The axial stress-strain curve of SCC3 samples under repeated uniaxial compressive loading

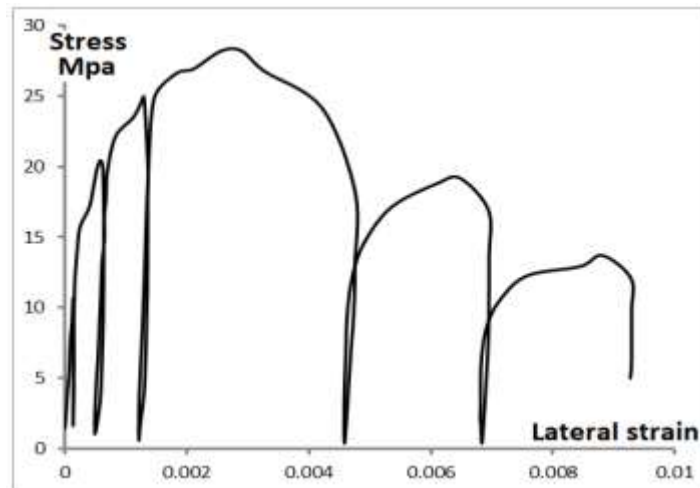


**Fig. 5:** The lateral stress-strain curve of SCC3 under compressive loading

In the stress-strain curve, the collision points of loading branch and unloading branch in each loading distances from one another as the number of loadings increases. The internal area of hysteresis loops increases as the uniaxial compressive loading increases until the maximum compressive points. This is due to higher energy absorption. After the peak point, demolitions decrease the absorption potential of the samples. Fig. 5 shows the lateral stress-strain curve of a fiber SCC under uniaxial compressive loading. This curve belongs to SCC3 sample introduced in Fig. 5. Strain results were calculated simultaneously. In fact, every stress has two strains which determine its Poisson's ratio at the same time. After the peak, the amount of lateral strain doubles.

Comparing the curves in Fig. 4 and .5, it is observed that the cracks are in such a direction that they absorb energy by opening and closing in the direction of compressive loading. In lateral direction, these cracks behave in a way that the interval between loading and permanent strains increases. In fact, in the lateral stress-strain curve, the transitive center-to-center strain of hysteresis loops increases as the number of loading increases.

As the lateral stress-strain curve of the SCC sample in uniaxial compressive loading shows, the loading and unloading branch is comprised of two linear and curved parts. The inner area of hysteresis loops is much lower than that of the axial curve and has lower energy absorption potential.

Comparison of the inner area of these two loops indicates that the ratio of the inner area of hysteresis loops for axial stress-strain curve is related to the square of the Poisson's ratio of the same load of uniaxial compressive loading.

### 3.3. Poisson's ratio

The analysis of the axial and lateral strain of the concrete sample under uniaxial compressive loading shows that Poisson's ratio changes non-linearly. The magnitude of these changes varies proportional to the compressive strength of the sample. As compressive strength increases, changes become more radical (Fig. 6).

Fig. 6 shows the variation curves of Poisson's ratio for uniaxial compressive loading of SCC1 to SCC4 with four different mixing fiber percentage. The additives in these mixing patterns are different. The variations in sample strength values are due to the increase in the compressive strength and tensile strength of concrete's mortar. The results show that initially the Poisson's ratios of SCC under compressive uniaxial compressive loading increases which is due to the variations in permanent strains in lateral strains. When deep cracks were made in the sample, and the stress increased to the concrete's maximum compressive strength, Poisson's ratio fell dramatically. However, after the dramatic fall in Poisson's ratio which is due to the increase in axial strain, it slightly increased.

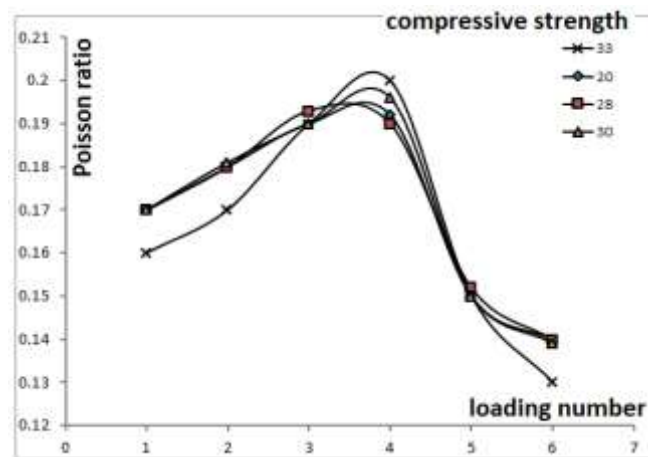


**Fig. 6:** The variations of Poisson's ratio curve for experiment samples

Before the sample breaks at the maximum compressive stress, the variation curve of Poisson's ratio has an uptrend. However, this uptrend pattern emerges again within the maximum compressive stress limit just after its dramatic fall. If the variations of the Poisson's ratio for SCC under uniaxial compressive loading are connected to a curve, an approximate concave-convex pattern will emerge. Afterwards, the Poisson's ratio for the number of loadings with  $f'_c$  stress falls within the limit of the turning point of the curve. Modeling and formulation are needed for a more accurate study of Poisson's ratio in uniaxial compressive loading because the changing behavior of Poisson's ratio depends on the way cracks are spread on the surface of the concrete and in its depth. Their spreading pattern depends on the relationship between the mortar and aggregates. Here, cracks pass either along the or within the aggregates which affects the whole seismic behavior of the structure.

### 4. Proposed model

The proposed model aimed at predicting the variations in the Poisson's ratio of SCC under various uniaxial compressive loadings. It predicts the Poisson's ratio of concretes in different loading numbers with respect to the maximum stress strength of the concrete and the number of loading numbers. Various models can be used for predicting the Poisson's ratio variations. This section however, aims at proposing a continuous model which makes a good approximation (Table 5).

**Table 5.** A model for predicting the Poisson's ratio variations of SCC samples

Limitation	Loading < 0.6f'c	0.6f'c < Loading < 1.3f'c	1.3f'c < Loading
	Elastic	Semi-elastic	Fracture zone
Number of loading	1 and 2	3 and 4	5 and 6
Poisson ratio	$v = (0.001 E - 0.02) * N + (-0.0008 F + 0.17)$	$v = (0.00022 E - 0.005) * N + (0.0001 F + 0.129)$	$v = (-0.0007 E + 0.009) * N + (0.0016 F + 0.11)$

**F = f'c/(1 MPa) ; E = Ec/(1 GPa) ; 25 MPa < Ec < 35 MPa ;  
N: fiber percentage ; Ec : elastic module ; f'c: compressive strength ;**

The proposed model makes a good approximation of Poisson's ratio variations. The highest discrepancies in models with laboratory results are within the maximum stress strength limit. As the compressive strength of the concrete increases, this difference slightly increases.

## 5. Conclusion

The Poisson's ratio of SCC depends on axial and lateral strains. These strains vary depending on the cracks made in the concrete. The repeated uniaxial compressive loading on SCC makes various cracks in their surface and depth. They spread in a way that they absorb the energy from loadings. It affects concrete behavior in axes perpendicular to loading axis and these behavioral changes were studied as variations in Poisson's ratio. The results of the present study are as followed:

- In increasing fiber percentage, Poisson's ratio increased before achieving the maximum compressive stress. This was due to the relative increase in lateral strain to axial strain. Moreover, Poisson's ratio decreased rapidly within the limit of the maximum compressive stress. It was due to the dramatic breaking of SCC and their deep cracks.
- The cracks made in SCC under uniaxial compressive uniaxial compressive loading are in a way that they absorb energy along the axis of loading and make permanent strains at the axis perpendicular to the axis of loading. The fiber protects crack wide and tension strength.
- The results show that an increase in fiber (only 2%) causes a significant increase in Poisson's ratio (more than 5%) after the second compressive loading.
- In repeated uniaxial compressive loading, Poisson's ratio changes dramatically as compressive strength increases by increasing fiber percentage.
- The ratio of the inner area of hysteresis loops in lateral stress-strain curve to those in axial stress-strain curve are proportional to the square of Poisson's ratio in the same number of loadings and after the peak point, the amount of lateral strain doubles.

## Reference

- Asprone D, Frascadore R, Ludovico MD, Prota A, Manfredi G. (2012), Influence of strain rate on the seismic response of RC structures. *Eng Struc*, 35, 29-36.
- Ayhan B, Jehel P, Brancherie D, Ibrahimbegovic A. (2013). Coupled damage–plasticity model for cyclic loading: Theoretical formulation and numerical implementation. *Eng Struc*, 50: 30-42.
- Azoti W.L, Koutsawa Y, Bonfoh N, Lipinski P, Belouettar S. (2013). Analytical modeling of multilayered dynamic sandwich composites embedded with auxetic layers. *Eng Struc*, 57, 248-253.
- Crambuer R, Richard B, Ile N, Ragueneau F. (2013) Experimental characterization and modeling of energy dissipation in reinforced concrete beams subjected to cyclic loading. *Eng Struc*, 56: 919-934.



- Cusatis, G. (2011). strain-rate effects on concrete behavior, international journal of impact engineering 38,162-170.
- Friis EA, Lakes RS, Park JB. (1988). Negative Poisson's ratio polymeric and metallic foams. J Materials Science, 23. 4406-4414.
- Gu, J., Wang, J., Lu, W. (2022). An experimental assessment of ultra-high-performance concrete beam reinforced with negative Poisson's ratio (NPR) steel rebar Construction and Building Materials 327, 127042.
- Huang, H., Yuan, Y., Zhang, W., Hao, R., & Zeng, J. (2020). Bond properties between GFRP bars and hybrid fiber-reinforced concrete containing three types of artificial fibers. Construction and Building Materials, 253, 111150.
- Lakes RS. (1987). Foam structures with a negative Poisson's ratio. Science 235, 1038-1040.
- Mi, P., Tan, P., Li, Y., Tang, M., Zhang, Y. (2023). Seismic behavior of steel reinforced precast concrete shear wall with replaceable energy dissipators. Structures, 56, 104972.
- Mohsenian Fard, E. Memar, M. Ghaedian, D. (2023). estimation on the Bond Behavior Between GFRP Bar and Polypropylene Fiber Reinforced Concrete with Pull-out Test. Civil and Project Journal, 5(4), 11-27
- Sideris KK, Manita P, Sideris K. (2004). Estimation of ultimate modulus of elasticity and Poisson ratio of normal concrete. Cem Conc Compo, 26: 623–631.
- Swamy R.N. (1971). dynamic Poisson ratio of Portland cement paste, mortar and concrete. Cem Concr Res, 1(5):559-583.
- Wang H, Qingbin Li Q. (2007). Prediction of elastic modulus and Poisson's ratio for unsaturated concrete. Int J Solids and Struc, 44:1370–1379.
- Wei, W., Liu, F., Xiong, Z., Lu, Z., & Li, L. (2019). Bond performance between fiber-reinforced polymer bars and concrete under pull-out tests. Construction and Building Materials, 220, 116133.
- Xie, H., Wei, P., Liu, N., Gao, J., Yang, L., Li, J., Chen. S. (2023). Study on failure characteristics of basalt fiber reactive powder concrete under uniaxial loading, Construction and Building Materials, 404, 133246.
- Zeng, J., Liao, J., Zhuge, Y., Guo, Y., Zhou, J., Huang, Z., Zhang. L. (2022). Bond behavior between GFRP bars and seawater sea-sand fiber-reinforced ultra-high strength concrete, Engineering Structures, 254, 113787.